

# Influence of the Environment on the Specificity of the Mg(II) Binding to Uracil

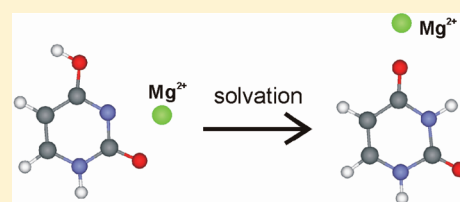
Ingrid Romancová,<sup>†</sup> Zdeněk Chval,<sup>\*,‡</sup> and Milan Předota<sup>†</sup>

<sup>†</sup>Institute of Physics and Biophysics, Faculty of Science, University of South Bohemia, Branišovská 31, CZ-370 05 České Budějovice, Czech Republic

<sup>‡</sup>Department of Laboratory Methods and Information Systems, Faculty of Health and Social Studies, University of South Bohemia, J. Boreckého 27, CZ-370 11 České Budějovice, Czech Republic

## S Supporting Information

**ABSTRACT:** Interactions of uracil with the  $\text{Mg}^{2+}$  ion were studied theoretically in the gas phase and in solution. The bare  $\text{Mg}^{2+}$  prefers bidentate N–C=O binding sites stabilizing rare keto–enol forms of the base. Hydration and/or phosphate binding of the  $\text{Mg}^{2+}$  ion shield its positive charge, which leads to preference of monodentate binding to the oxygen keto atoms, shifting fully the equilibrium between the tautomers back toward the canonical diketo tautomer. In solution, a direct inner-sphere metal binding to uracil is not clearly advantageous compared to the outer-sphere metal binding. Similar trends were also obtained for the  $\text{Ca}^{2+}$  ion. Results are supported by the natural bond orbital (NBO) and atoms in molecule (AIM) analyses and the combined extended transition-state energy decomposition analysis and natural orbitals for chemical valence (ETS-NOCV).



## INTRODUCTION

Metal ion–nucleobase interactions are recognized as fundamental with respect to changes in the nucleic acid structure stabilizing a number of local motifs. This is especially important for complicated RNA structures in which metal ions ensure their proper folding. Uracil is a specific base for RNA in which it pairs up with adenine. All nucleobases including uracil may exist in different tautomeric forms, and this behavior may have important biological consequences, such as point mutations<sup>1,2</sup> because the mispairs of DNA bases can be stabilized by metalation.<sup>3–6</sup> In case of RNA, the rare tautomers may be stabilized by specific tertiary interactions, and they may take part in ribozyme catalysis. Tautomeric equilibria of the nucleobases were studied in a number of previous studies in the gas phase and in aqueous solution.<sup>7–12</sup> The metal ions may shift the tautomeric equilibria toward to rare enol tautomers mainly in the case of isolated adenine and thymine, while for cytosine, this event is not probable.<sup>13</sup> In the case of guanine, the rare tautomers can coexist when the base is isolated; however, their formation is suppressed in the case of strong interactions between the metal ion and the phosphate group.<sup>14</sup>

The other factor that affects the chemical equilibrium between tautomers is the surrounding environment.<sup>15</sup> Water molecules may significantly change the relative stabilities of tautomers compared to the gas phase and nonpolar solvents. For example, the enol form of cytosine is the most stable tautomer in the gas phase, but its canonical form is more stable in water because it is much better stabilized; hydration by just two water molecules is sufficient for this stabilization.<sup>16</sup> Water as a polar solvent better stabilizes the tautomers with a larger

dipole moment and may shield unfavorable electrostatic interactions.<sup>17</sup>

Beside the phosphate oxygens, the main metal binding sites of the metals on nucleobases are N7 and N3 atoms of purines, O6 of guanine, and oxo groups of pyrimidines. Stabilization of rare nucleobase tautomers by metal ions was studied extensively<sup>13,18–23</sup> as well as the influence of the metal ions on the base pairing.<sup>24–29</sup> For a complex of the  $\text{Mg}^{2+}$  ion with uracil, the most favored binding motif in the gas phase is  $\text{N}\cdots\text{Mg}^{2+}\cdots\text{O}$ .<sup>21</sup> Because the canonical form of uracil offers only the monodentate binding motif, the rare enol tautomers, which offer bidentate binding sites, are expected to be stabilized in the presence of a metal ion. For example Wang et al.<sup>30</sup> studied uracil interactions with the  $\text{Zn}^{2+}$  ion. In the most stable structure, the  $\text{Zn}^{2+}$  ion binds in the bidentate manner to N1 and O2 atoms. The canonical tautomer with the metal bound to O4 is by 22.4 kcal/mol less stable. Monohydration of the  $\text{Zn}^{2+}$  ion decreases the difference between the two binding modes by one-third to the value of 15.0 kcal/mol.<sup>30</sup> In the gas phase, a monodentate  $\text{Mg}^{2+}$  binding to thymine may at first activate the 1,3 hydrogen transfer, which is followed by the metal cation migration to form a bidentate complex,<sup>31</sup> stabilizing a rare tautomer. The speed of the hydrogen transfer can be substantially increased if at least one water molecule is involved in the reaction mechanism.<sup>32,33</sup>

On the other hand, monovalent metal ions probably are not able to stabilize the rare tautomers. For example, adducts of the

Received: September 13, 2011

Revised: January 13, 2012

Published: January 20, 2012

$\text{Li}^+$  ion with the uke2 keto–enol tautomer (equivalent to uke2–O+w and uke2–ON+w (Figure 1)) were, respectively,

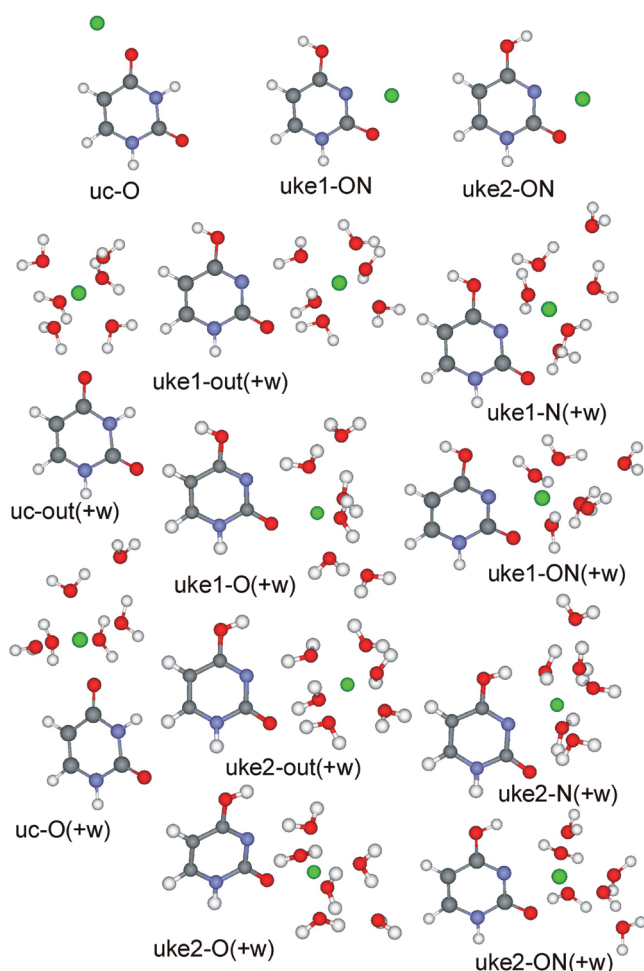


**Figure 1.** Optimized complexes of the  $\text{Mg}^{2+}$  ion that belong to the  $\text{U}+\text{M}$  (the upper part) and  $\text{U}+\text{M}+6\text{W}$  systems (the lower part). Structures are designated according to the uracil tautomer (uc = diketo canonical tautomer; uke1 and uke2 = keto–enol rare tautomers) and a metal's binding mode (out = outer-sphere binding of uracil; O = binding to the keto oxygen (O2 or O4); N = binding to N3; ON = bidentate binding to O2 and N3). The part of the name in parentheses is used in the text and Table 4, but not in Tables 1–3, where the name of the system is used to distinguish between the same structures that belong to different systems. Only the most stable conformer of each structure is shown.

by 12.8 and 15.2 kcal/mol less stable than the complex with the canonical uc tautomer (equivalent to uc–O+w (Figure 1) in the gas phase and when only one water ligand from the metal coordination shell was considered.<sup>34</sup>

In case of the  $\text{Cu}^{2+}$  ion, the interaction with uracil is more complex than that for the divalent ions studied here. The rare tautomers will not be stabilized in the  $(\text{Cu}–\text{uracil})^{2+}$  system as the most stable adduct is formed with the canonical forms of uracil and thymine even for the bare  $\text{Cu}^{2+}$  ion in the gas phase.<sup>19,35</sup> However,  $\text{Cu}^{2+}$  is a strong oxidizing agent<sup>36–39</sup> forming a  $\text{Cu}^+–\text{U}^+$  type of complex.<sup>37</sup> It promotes a deprotonation of the N3 nitrogen and stabilization of the bidentate N3 and carbonyl oxygen adduct (at least in the gas phase).<sup>40</sup>

Description of the binding of the metal ions in solution is more complicated because an establishing a direct coordination bond of the nucleobase to the metal is connected with the exchange for one (monodentate binding) or two (bidentate binding) water ligands. When calculating energetic feasibility of this process, one should consider the specific environment of the metal ion because it influences the strengths of metal ions' coordination bonds. In the case of nucleobases, the metal ion binding to a negatively charged backbone phosphate group can be expected.<sup>41</sup> This interaction may suppress the likelihood of the rare tautomer formation.<sup>14</sup>

The importance of the solvent effects on the relative stability of the uracil tautomers complexed with  $\text{Pt(II)}$  compounds was already stressed by Lippert and co-workers.<sup>42</sup> Although the  $\text{Pt(II)}$  complexes with uracil are also usually deprotonated to  $\text{U}^-$ , forming the  $\text{Pt}–\text{N3}$  bond,<sup>42,43</sup> it was shown that stabilization of rare tautomers of uracil in  $\text{Pt(II)}$  complexes may occur even for neutral uracil in solution and it is caused by a preferential binding to the N3 atom over O2 and O4.<sup>42</sup>

Metal interactions with uracil and its derivatives were studied in a number of theoretical and experimental studies.<sup>22,30,32,40,44–53</sup> However, to the best of our knowledge, there is not any systematic study dealing with uracil interactions with the  $\text{Mg}^{2+}$  ion, which is the most relevant divalent metal cation in vivo. The current paper extends the study of Russo et al.<sup>21</sup> in which three possible complexes of uracil tautomers with the bare  $\text{Mg}^{2+}$  ion were compared and the study of Kabeláč and Hobza, where interactions of bare metal ions  $\text{Na}^+$  and  $\text{Mg}^{2+}$  with DNA nucleobases were studied systematically.<sup>13</sup> Unlike the cited studies, we also study in detail the influence of environmental effects, such as the presence of the metal ion's hydration shell, of bulk water, and of the phosphate group, on the specificity of the binding of the metal ion. For the sake of simplicity, these effects are usually neglected in most theoretical studies.

Finally, the relevant complexes of the bare/hydrated  $\text{Mg}^{2+}$  ion with uracil were reoptimized also for the  $\text{Ca}^{2+}$  ion, and differences resulting from the different behavior of the two ions were discussed.

## ■ COMPUTATIONAL METHODS

Starting geometries of all structures were generated with the MOLDEN program,<sup>54</sup> and calculations were performed with the Gaussian 09 (G09) program package.<sup>55</sup> The DFT/B3LYP method was used for both geometry optimizations and single-point calculations. Calculation of each structure was done in three steps: (i) every structure was preliminarily optimized with the 6-31+G\* basis set and also the nature of the obtained stationary points was checked by a vibrational analysis. Thermal contributions to the energetic properties were calculated using the canonical ensemble of statistical mechanics at standard conditions ( $T = 298 \text{ K}$ ,  $p = 101.325 \text{ kPa}$ ). (ii) Final geometry optimizations were performed with the more flexible 6-311++G\*\* basis set in both the gas phase and in solution. (iii) Single-point energy evaluations on the final optimized geometries were carried out with the 6-311++G(2df,2pd) basis set. Default PCM parametrization as implemented for water in G09 was used in all solution-phase calculations. The calculated electron densities on this level of theory were used for natural bond order (NBO) and atoms in molecule (AIM) analyses. AIM analyses were performed by the AIMALL program.<sup>56</sup>

Structures with one or two  $\text{H}_2\text{O}$  ligands in the second coordination shell have more possible conformers, differing in

the position of the outer-sphere ligand(s). Because we are interested in the changes of relative energies upon different modes of  $\text{Mg}^{2+}$  ion binding, we considered only structures in which the outer-sphere water ligand(s) interacted only with the inner-sphere water or phosphate ligands, while structures with direct contacts of the outer-sphere water ligand(s) with uracil were discarded. It decreased the number of possible conformers.

Interaction energies were computed as the differences between the total energies of the complexes and the energies of the isolated monomers and have been corrected for deformation energies and the basis set superposition error (BSSE) using the standard counterpoise method.<sup>57</sup> In the calculations of BSSE corrections within the PCM regime, the ghost atomic orbital functions were localized inside of the cavity, which has the same size as the whole complex, as was described previously by Zimmermann and Burda.<sup>58</sup>

Additional single-point calculations on selected G09-optimized structures were conducted using the Amsterdam density functional 2010.01 package (ADF)<sup>59</sup> to calculate fragment energy decompositions according to the extended transition-state theory<sup>60,61</sup> and to perform bond analysis using the combined extended transition-state energy decomposition analysis and natural orbitals for chemical valence (ETS-NOCV).<sup>62–64</sup> In these calculations, a triple- $\zeta$  STO basis set was used, with two sets of polarization functions as provided in the ADF.

## RESULTS AND DISCUSSION

We compared relative energies of uracil tautomers (U) in the presence of (1) a bare  $\text{Mg}^{2+}$  cation in the gas phase (the system U+M), (2) the hexahydrated  $\text{Mg}^{2+}$  cation (the system U+M+6W) in both the gas phase and continuum water environment (Figure 1), and (3) the hydrated  $\text{Mg}^{2+}$  ion with a coordinated phosphate anion (the system U+M+5W+P) in both the gas phase and continuum water environment (Figure 2). By this, we were able to evaluate quantitatively the influence of the ion coordination (inner and outer) and of the environment on the equilibrium between the tautomers.

**1. Gas-Phase Environment. U+M System.** Interaction and relative energies of structures of the U+M system are depicted in Table S1 (Supporting Information) and are compared with interaction energies for the thymine– $\text{Mg}^{2+}$  system. Interaction energies for the uracil are systematically by about 4–5 kcal/mol less negative than those for thymine.

The most favorable structures are formed by the  $\text{Mg}^{2+}$  interactions with keto–enol uracil (uke) tautomer(s) that exhibit a bidentate  $\text{N}\cdots\text{Mg}^{2+}\cdots\text{O}(\text{keto})$  binding motif, the  $\text{N3}\cdots\text{Mg}^{2+}\cdots\text{O2}(\text{keto})$  motif being the most stable (structure uke1–ON; see Figure 1 and Table S1, Supporting Information). The metal complex with the canonical form of uracil (uc) enables only monodentate  $\text{Mg}^{2+}\cdots\text{O}(\text{keto})$  binding motifs. The one with the  $\text{Mg}^{2+}\cdots\text{O4}(\text{keto})$  binding motif (structure uc–O) represents energetically the seventh structure, being less stable by 22.1 kcal/mol than the uke1–ON structure. This is in reasonable agreement with the study of Russo et al.<sup>21</sup> considering that uc–O, uke2–ON, and uke5–ON structures (Table 1 and Table S1, Supporting Information) were compared in the cited study. Note that in the absence of the metal ion, the canonical diketo uc tautomer is by at least 10 kcal/mol more stable than any other possible isomer (cf. Table 1).<sup>15,42,65,66</sup>

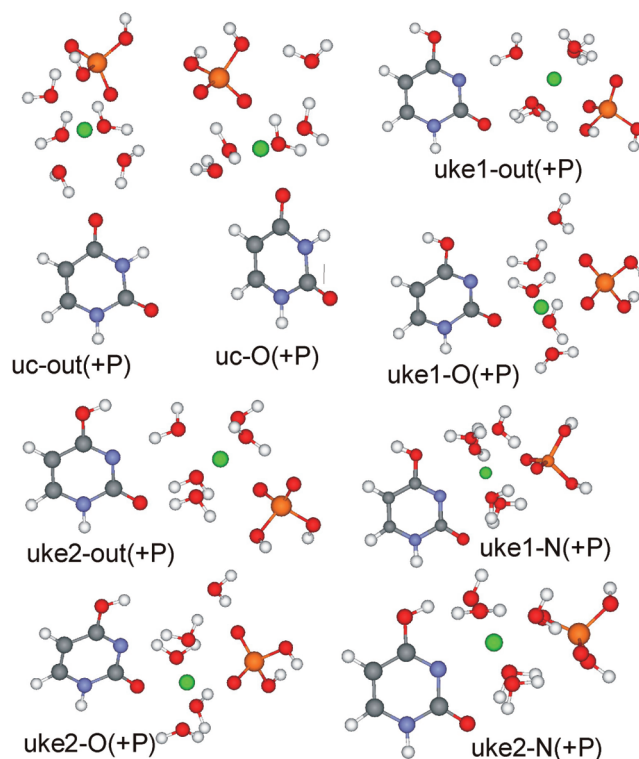


Figure 2. Optimized complexes of the  $\text{Mg}^{2+}$  ion that belong to U+M+5W+P system. See Figure 1 for further description.

Table 1. Dependence of Relative Free Energies (in kcal/mol) of the uc, uke1, and uke2 Tautomers on the Surroundings of the Bound  $\text{Mg}^{2+}$  Ion<sup>a</sup>

structure/ system	U		U+M	U+M+6W		U+M+5W+P	
	gas phase	PCM	gas phase	gas phase	PCM	gas phase	PCM
uc-out	0.0	0.0	n.a.	3.3	1.6	1.5	2.0
uc-O			0.0	0.0	0.0	0.0	0.0
uke1-out	17.7	12.7	n.a.	2.9	11.0	11.5	12.9
uke1-O			n.a.	-3.2	8.4	6.9	9.9
uke1-N			n.a.	7.8	14.2	13.3	14.9
uke1-ON			-22.1	0.4	11.9	n.s.	n.s.
uke2-out	11.6	10.9	n.a.	5.4	10.5	10.5	12.2
uke2-O			n.a.	-2.2	7.4	4.3	8.4
uke2-N			n.a.	10.7	12.9	11.7	15.6
uke2-ON			-16.5 <sup>b</sup>	3.9	11.2	n.c.	n.c.

<sup>a</sup>n.s. = not stable structure, see the text; n.a. = structure is not available; n.c. = not considered, see the text. <sup>b</sup>A relative energy  $\Delta E_{\text{ZPE}}$  of –17.4 kcal/mol was calculated in ref 21.

**U+M+6W System.** In the water environment, the  $\text{Mg}^{2+}$  ion is surrounded by water ligands, which can be exchanged for electronegative groups of biomolecules if it is energetically feasible. Water ligands on the one hand screen the charge of the  $\text{Mg}^{2+}$  ion, decreasing electrostatic forces between the metal and uracil; on the other hand, additional H-bond interactions between the water molecules and uracil may be formed. Thus, interaction of uracil with the hydrated  $\text{Mg}^{2+}$  ion is a more complex event than uracil interaction with the bare  $\text{Mg}^{2+}$  ion.

The goal of this study is to show dependence of the specificity of the  $\text{Mg}^{2+}$  ion's binding to uracil on its environment, especially with respect to the monodentate/bidentate binding because it is directly related to the



tautomerism of uracil. Therefore, we have not calculated relative stabilities of all possible metal binding sites with all uracil tautomers as was done for the bare  $\text{Mg}^{2+}$  ion. For the  $\text{U}+\text{M}+6\text{W}$  system, the seven most stable structures of the  $\text{U}+\text{M}$  system (Table S1, Supporting Information) were hydrated by six water molecules<sup>67</sup> considering the following types of structures: (1) structures in which the hydrated  $\text{Mg}^{2+}$  ion interacts with the uracil isomer only via hydrogen bonds, that is, the uracil molecule is in the second coordination shell of the  $\text{Mg}^{2+}$  ion (structures  $\text{uc-out}+\text{w}$  and  $\text{uken-out}+\text{w}$ ,  $n = 1-6$ ) and (2) structures with a monodentate  $\text{Mg}^{2+}$  coordination to the keto-oxygen (structures  $\text{uc-O}+\text{w}$  and  $\text{uken-O}+\text{w}$ ,  $n = 1-6$ ). Two other types of complexes are possible for the  $\text{uken}$  enol-keto tautomers: (3) monodentate  $\text{Mg}^{2+}$  coordinated structures and (4) bidentate  $\text{Mg}^{2+}$  coordinated structures, wherein the metal is coordinated only to the N3 atom of uracil (structures  $\text{uken-N}+\text{w}$ ) and to O2 and N3 atoms (structures  $\text{uken-ON}+\text{w}$ ). The most stable complexes with the metal are formed by the  $\text{uke1}$  and  $\text{uke2}$  keto-enol tautomers and by the canonical  $\text{uc}$  tautomer (Table 1). In the subsequent text, we will concentrate on the description of the energy changes between the complexes of these three tautomers. Relative energies of metal complexes of  $\text{uke3-6}$  tautomers are shown in Table S2 (Supporting Information).

In the gas phase, the energy gap of 22.1 kcal/mol calculated between the most stable  $\text{uke1-ON}$  structure (within the  $\text{U}+\text{M}$  system) and the canonical  $\text{uc-O}$  structure almost fully diminished in the  $\text{U}+\text{M}+6\text{W}$  system. The most stable  $\text{uke1-O}+\text{w}$  structure is only lower than the  $\text{uc-O}+\text{w}$  canonical structure by 3.2 kcal/mol (Table 1). The former structure is stabilized mainly by electrostatic interactions (−84.6 kcal/mol, Table S3, Supporting Information). Orbital interactions can be decomposed to (1)  $\sigma$ -electron polarization, which strongly contributes to  $\text{Mg-O2}$  bonding (−15.7 kcal/mol, Table S3, Supporting Information) and H-bonding (−10.0 kcal/mol) and (2)  $\pi$ -electron polarization (−11.2 kcal/mol). The most important deformation density contributions belonging to these effects are shown in Figure 3. In the gas phase, the strength of these interactions compensates for the penalty of 17.7 kcal/mol needed for the diketo  $\rightarrow$  keto-enol tautomerization. An exchange of a water ligand for the N3 nitrogen is not energetically feasible due to the well-known magnesium preference for oxygen over nitrogen binding.<sup>68</sup>

Explicit inclusion of the first metal's coordination shell relatively destabilizes the bidentate  $\text{uke1-ON}+\text{w}$  structure (with the  $\text{N3-Mg-O2}$  binding motif). Formation of the  $\text{Mg-N3}$  bond at the expense of breaking of the  $\text{O4}\cdots\text{HOH}(\text{Mg})$  H-bond is connected with an energy gain of only 0.4 kcal/mol (Figure 1, Table S3, Supporting Information); however, the change in the  $\pi$ -electron polarization contribution makes the  $\text{uke1-ON}+\text{w}$  structure less stable by 3.6 kcal/mol than the monodentate structure  $\text{uke1-O}+\text{w}$  (with the  $\text{Mg-O2}$  bond). Therefore, the bidentate structures should not be detected in solution, and a hydrogen transfer from the N3 to O4 keto group, which leads to formation of the keto-enol tautomer (and which might be facilitated in the presence of water molecules<sup>47,69-72</sup>), cannot be expected to activate the metal chelation process, as was observed for the bare metal ion in the gas phase.<sup>73</sup>

Electron densities at bond critical points (BCPs) between the metal and uracil are decreased by 45 and 40% when the metal ion in the  $\text{uco-O}$  and  $\text{uke-ON}$  structures is hydrated to form the  $\text{uc-O}+\text{w}$  and  $\text{uke-ON}+\text{w}$  structures, respectively (Table

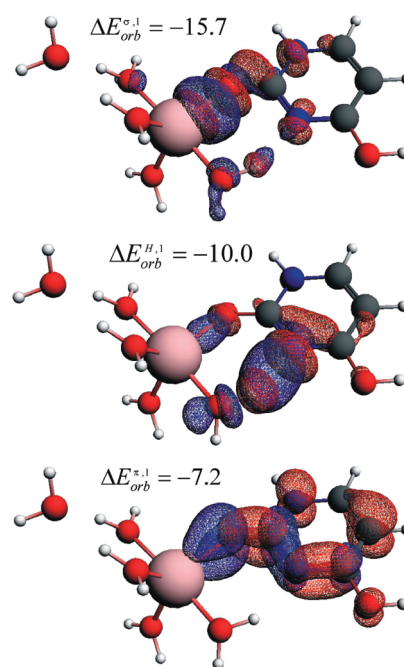


**Figure 3.** The contours of three most important deformation density contributions  $\Delta\rho_{\sigma,1}$ ,  $\Delta\rho_{\pi,1}$ , and  $\Delta\rho_{\text{H},1}$  describing the interaction of the uracil fragment with the hydrated  $\text{Mg}^{2+}$  ion in the  $\text{uke1-O}+\text{w}$  structure. In addition, the corresponding ETS-NOCV-based energies (in kcal/mol) are shown. Total interaction energies assigned to  $\sigma$ -bonding,  $\pi$ -electron polarization and to H-bonding are shown for selected structures in Table S3 (Supporting Information). The contour values are  $\pm 0.001$  au. The blue/red contours correspond to accumulation/depletion of electron density.

S4, Supporting Information). However, the interaction energies are decreased more than three times for both systems after inclusion of the first hydration shell (Table 2). It refers to a

**Table 2.** Gas-Phase and Solvent-Phase Interaction Energies (in kcal/mol, Corrected for the Deformation Energies and BSSE Error) of the Uracil Tautomers with the  $\text{Mg}^{2+}$  Ion and Its Environment (Explicit Water Molecules and the Phosphate)

structure/system	U+M	U+M+6W		U+M+5W+P	
	gas phase	gas phase	PCM	gas phase	PCM
uc-out	n.a.	−36.3	−9.4	−21.1	−9.4
uc-O	−130.47	−38.5	−9.9	−20.4	−9.2
uke1-out	n.a.	−57.4	−15.5	−32.1	−14.5
uke1-O	n.a.	−63.1	−19.3	−34.6	−15.4
uke1-N	n.a.	−51.4	−11.5	−29.0	−11.1
uke1-ON	−170.95	−55.5	−10.5	n.s.	n.s.
uke2-out	n.a.	−48.3	−13.8	−26.6	−13.1
uke2-O	n.a.	−57.0	−15.5	−30.6	−14.6
uke2-N	n.a.	−43.8	−13.9	−26.0	−10.3
uke2-ON	−158.4	−48.9	−12.0	n.c.	n.c.

basically electrostatic nature of the  $\text{Mg-O}$  and  $\text{Mg-N}$  bonds in the  $\text{uco-O}$  and  $\text{uke-ON}$  structures with an unscreened  $\text{Mg}^{2+}$  charge. Moreover, it has to be stressed that the Laplacian of the electron density at BCP  $\nabla^2\rho_{\text{BCP}}$  is positive for all  $\text{M}^{2+}$ –uracil interactions in all structures discussed in this study, which refers to ionic nature of  $\text{M}^{2+}$ –uracil bonds.

Table 3. Bond Distances (in Å) of Structures Optimized in the Gas Phase (Upper Values) and in the Solvent (Lower Values)<sup>a</sup>

structure/bond	Mg–O2	Mg–N3	Mg–O4	H-bonds	Mg–O2	Mg–N3	Mg–O4	H-bonds
<b>U+M+6W</b>					<b>U+M+5W+P</b>			
uc-out				1.675 <sup>d</sup> ; 1.695 <sup>d</sup> 1.754 <sup>d</sup> ; 1.782 <sup>d</sup>				1.764 <sup>d</sup> ; 1.872 <sup>d</sup> 1.771 <sup>d</sup> ; 1.803 <sup>d</sup>
uc–O			2.013 2.038				2.069 2.073	
uke1-out				1.797 <sup>b</sup> ; 1.800 <sup>b</sup> ; 1.777 <sup>c</sup> 1.821 <sup>b</sup> ; 1.826 <sup>b</sup> ; 1.796 <sup>c</sup>				1.950 <sup>b</sup> ; 1.958 <sup>b</sup> ; 1.852 <sup>c</sup> 1.833 <sup>b</sup> ; 1.881 <sup>b</sup> ; 1.806 <sup>c</sup>
uke1–O	2.012 2.036			1.873 <sup>c</sup> 1.868 <sup>c</sup>	2.106 2.089			2.010 <sup>c</sup> 1.903 <sup>c</sup>
uke1–N		2.352 2.309		1.855 <sup>b</sup> ; 1.899 <sup>b</sup> ; 2.205 <sup>d</sup> 2.073 <sup>b</sup> ; 2.033 <sup>b</sup> ; 2.152		2.414 2.378		1.892 <sup>b</sup> ; 2.185 <sup>d</sup> 1.792 <sup>b</sup> ; 2.070 <sup>d</sup>
uke1–ON	2.142 2.262	2.343 2.245		2.893 <sup>d</sup> 2.397 <sup>d</sup>				
uke2-out				1.765 <sup>b</sup> ; 1.784 <sup>b</sup> ; 1.869 <sup>c</sup> 1.807 <sup>b</sup> ; 1.834 <sup>b</sup> ; 1.863 <sup>c</sup>				1.897 <sup>b</sup> ; 1.987 <sup>b</sup> ; 1.887 <sup>c</sup> 1.840 <sup>b</sup> ; 1.868 <sup>b</sup> ; 1.867 <sup>c</sup>
uke2–O	1.999 2.029			1.928 <sup>c</sup> 1.936 <sup>c</sup>	2.095 2.085			2.034 <sup>c</sup> 1.955 <sup>c</sup>
uke2–N		2.186 2.269		2.158 <sup>b</sup> ; 2.319 <sup>b</sup> ; 2.054 <sup>e</sup> 1.854 <sup>b</sup> ; 2.317 <sup>b</sup> ; 1.779 <sup>e</sup>		2.263 2.294		2.062 <sup>b</sup> ; 2.363 <sup>b</sup> ; 1.830 <sup>e</sup> 1.950 <sup>b</sup> ; 2.130 <sup>b</sup> ; 1.778 <sup>e</sup>
uke2–ON	2.297 2.301	2.400 2.190		— 1.971 <sup>c</sup>				

<sup>a</sup>See Table S4 (Supporting Information) for electron densities at BCPs. In the U+M system, the bonding distance Mg–O4 is 1.795 Å for the uc–O structure. Mg–O2 and Mg–N3 distances are 1.967 and 2.089 Å and 1.945 and 2.135 Å for the uke1–ON and uke2–ON structures, respectively.

<sup>b</sup>O2...HOH hydrogen bond. <sup>c</sup>N3...HOH hydrogen bond. <sup>d</sup>O4...HOH hydrogen bond. <sup>e</sup>O4H...OH<sub>2</sub> hydrogen bond

NBO analysis shows that a mean transferred charge to Mg<sup>2+</sup> is about –0.1 e per ligand for the U+M+6W system in the gas phase. This value is almost independent of the number and the size of the ligands, being roughly the same for all structures in both the U+M and U+M+6W systems with the same coordination number, that is, magnesium has NPA charges of ~1.5 and ~1.4 e when it is, respectively, penta- and hexa-coordinated (Table S5, Supporting Information). Looking at the charges of the uc-out and uke1(2)-out structures in Table S5 (Supporting Information), one can also see an indirect charge flow from uracil to the metal ion via H-bonded water ligands (cf. Figure 3).

**U+M+5W+P System.** In nucleic acids, the sugar–phosphate backbone is the main target of the Mg<sup>2+</sup> ions. Direct phosphate–uracil contacts cannot be observed in nucleic acids (at least at physiological pH) but have to be mediated by metal ions and/or water molecules. To study the influence of electrostatic screening of the phosphates on the specificity of the metal ion binding to uracil, the inner-sphere water ligand, which is in the trans position with respect to the bound uracil, was replaced by the phosphate H<sub>2</sub>PO<sub>4</sub><sup>–</sup> anion. This arrangement ensured that no direct contacts between the phosphate and uracil groups might be established during optimizations. Of course, this arrangement does not represent a realistic model of uridine monophosphate (or an intranucleotide macrochelate) because we completely neglected the sugar linkage. However, in a real RNA environment, the uracil base and the phosphate group bound by the same metal do not need to belong to the same nucleotide, forming an internucleotide macrochelate.<sup>74</sup> Note that the Mg<sup>2+</sup> ion may also bind the phosphate anion in the outer-sphere manner. This situation is not described in this study due to a large number of possible energetically close conformers, but its influence on tautomer stabilization can be estimated considering U+M+6W and U+M+5W+P as the boundary systems.

The presence of the phosphate anion in the metal's first coordination shell further destabilizes the bidentate uke–ON +P structure, which does not exist as a minimum always being transferred to the monodentate uke–O+P structure upon optimization. On the other hand, the uke2–ON+P structure is stable but only due to a direct phosphate–uracil O4H...OP interaction. Therefore, the stability of uke2–ON+P is overestimated with respect to the other structures (where the direct phosphate–uracil interactions are avoided; see above), and therefore, we do not consider this structure here.

In the U+M+5W+P system, the gas-phase results already predict a higher stability of the uc complexes than of the rare tautomer uke1 and uke2 complexes but still overestimates the stability of the latter complexes with respect to the results for the solvent environment (Table 1). In the gas phase, the presence of a negatively charged phosphate decreases the values of interaction energies to less than two-thirds (by 37 ± 2%) with respect to the values calculated for the U+M+6W system (Table 2). Note that the same effect was already observed in the inverse sense; the inner-shell binding of the metal to guanine substantially reduced the strength of the (outer-shell) metal binding to the phosphate group.<sup>75</sup>

Because the metal–uracil interactions are governed mainly by electrostatics, we decided to analyze the changes in the interaction energies upon phosphate binding (i.e., when reducing the charge of the metal fragment from +2 to +1 e). According to the energy decomposition analysis, a drop of energies of orbital interactions covers more than 50% of the total decrease of interaction energies caused by a phosphate binding because a decrease of the electrostatic energy is partly compensated for by a decrease of the Pauli repulsion (Table S3, Supporting Information). ETS-NOCV analysis of orbital interactions shows that the presence of the phosphate decreases mainly energy contributions connected with a polarization of  $\pi$ -electrons of the uracil aromatic ring (by ~70%), the energy of

H-bonds (by  $\sim 40\%$ ), and, to the least extend, the energy of the direct  $\text{Mg}^{2+}$ –uracil interactions (by  $\sim 20\%$ ) connected with the redistribution of the  $\sigma$ -electrons (Figure 3 and Table S3, Supporting Information).

These results are in agreement with the AIM analysis (Table S4, Supporting Information); the phosphate binding does not change the strengths of  $\text{Mg}$ – $\text{OH}_2$  interactions but decreases the strength of H-bond interactions between uracil and water ligands (by at least 25%) and also slightly that of direct  $\text{Mg}$ –uracil interactions (by at least 10%).

Substitution of one water ligand in the first coordination shell for the phosphate group lowers the metal's charge only by about 0.03e. The phosphate group has the total charge of about  $-0.79\text{e}$  (Table S3, Supporting Information). The transferred negative charge is uniformly spread over the system, and the total charges of the other metal's ligands (including uracil) are decreased also by about 0.03 e per ligand (i.e., by the same value as the metal). A water environment decreases the charge transfer from the phosphate group by about 10% (cf. results in the next section).

**2. Water (Solvent-Phase) Environment.** The water environment affects the geometries of the optimized structures to some extent; it especially tends to shorten the H-bonds (Table 3). The electron densities at BCPs of these H-bonds are increased accordingly, which may increase their relative strengths with respect to the direct  $\text{Mg}$ – $\text{O}/\text{Mg}$ – $\text{N}$  interactions in solution. However, the nature of all H-bond interactions remains strongly ionic ( $\nabla^2\rho_{\text{BCP}} > 0$ ); therefore, their real absolute strengths are governed by electrostatics. For example, in  $\text{uc-O+w}$ , the metal fragment interacts with uracil only via two H-bonds, which are shortened by about 0.08 Å in solution (Table 3), but at the same time, the interaction energy between the fragments is decreased almost four times (Table 2).

The water environment has a profound effect on the relative energies of the complexes. The canonical  $\text{uc-O+w}$  structure is by 8.4 and 7.4 kcal/mol more stable than the  $\text{uke-O+w}$  and  $\text{uke2-O+w}$  structures, respectively (Table 1). The  $\text{uke2}$  tautomer complexes are systematically more stable by about 1–2 kcal/mol than the  $\text{uke1}$  ones. Inclusion of the implicit solvent leads to even larger destabilization of the complexes with the bidentate bonding of the metal represented by the  $\text{uke-ON+w}$  and  $\text{uke2-ON+w}$  structures; they are by 11.9 and 11.2 kcal/mol, respectively, less stable than the  $\text{uc-O+w}$  structure. Therefore, in solution, the formation of the rare tautomers of uracil with a bound  $\text{Mg}^{2+}$  ion should be completely suppressed.

There is only a slight free-energy gain upon the direct metal coordination to uracil with respect to the outer-sphere binding because the difference between the  $\text{uc-O+w}$  and  $\text{uc-out+w}$  structures is only 1.6 kcal/mol. The O4 atom of the canonical form is the main metal's binding site in uracil. In solution, one can expect a similar probability for its inner- and outer-sphere binding by the  $\text{Mg}^{2+}$  ion. This finding is in accord with experimental observations.<sup>74</sup>

The solvation diminishes differences in interaction energies between the uracil and metal fragments in the structures of the  $\text{U+M+6W}$  and  $\text{U+M+5W+P}$  systems. Compared to the gas phase, the lowering of the interaction energies in the +2 charged structures of the  $\text{U+M+6W}$  system is more than two times higher than that in the +1 charged structures of the  $\text{U+M+5W+P}$  system. It refers to the importance of the electrostatic stabilization of the gas-phase structures.

In solvent, the relative energies of the  $\text{U+M+5W+P}$  structures are in qualitative agreement with the results for the  $\text{U+M+6W}$  system, but still, the presence of the phosphate in the first coordination shell destabilizes systematically the keto–enol tautomers by about 2 kcal/mol (Table 1). Therefore, the phosphate group enhances the protective and shielding effects of the water environment against the possible shifts of tautomeric equilibria caused by metal ions, as suggested already for the metal binding to guanine.<sup>14</sup>

The water environment decreases the polarization of the uracil and also very slightly the charge transfer from the uracil fragment toward the hydrated metal fragment. The changes of the NPA charges of the atoms on the uracil fragment can be up to the order of several tenths of the elementary charge (e) decreasing the polarization of uracil by more than 50% for all the structures. The changes in the transferred charges are on the order of 0.01 e, reducing the charge transfer but only by less than 10% for most of the structures.

**3. Comparison with the  $\text{Ca}^{2+}$  Ion.** We performed optimizations of the structures in the  $\text{U+M}$  and  $\text{U+M+6W}$  systems also with the  $\text{Ca}^{2+}$  ion. The  $\text{Ca}^{2+}$  ion forms weaker interactions with uracil than the  $\text{Mg}^{2+}$  ion. For structures in the  $\text{U+M}$  system, interaction energies with uracil are smaller for the  $\text{Ca}^{2+}$  ion than for the  $\text{Mg}^{2+}$  ion by about 20%. The water ligands ( $\text{U+M+6W}$  system) decrease this relative difference down to  $\sim 10\%$  mainly due to a higher flexibility of the  $\text{Ca}^{2+}$  hydration shell (cf. gas-phase interaction energies corrected for deformation energies in Tables 2 and 4 with the uncorrected

**Table 4. Relative Gibbs Free Energies (in kcal/mol) of the Structures in the  $\text{U+M}$ ,  $\text{U+M+6W}$  Systems Stabilized by the  $\text{Ca}^{2+}$  Ion Together with Interaction Energies (Corrected for the Deformation Energies and BSSE) between the Uracil and Metal Fragments<sup>a</sup>**

	$\Delta G$		$\Delta E_{\text{int}}$	
	gas phase	PCM	gas phase	PCM
$\text{uc-O}$	0.0		−106.9	
$\text{uke1-ON}$	−10.6		−136.5	
$\text{uke2-ON}$	−5.5 <sup>b</sup>		−124.8	
$\text{uc-out+w}$	3.3	−0.6	−34.2	−9.0
$\text{uc-O+w}$	0.0	0.0	−38.3	−9.2
$\text{uke1-out+w}$	4.8	10.0	−53.7	−14.5
$\text{uke1-O+w}$	0.3	8.9	−57.5	−16.1
$\text{uke1-N+w}$	n.s.	11.9	n.s.	−13.2
$\text{uke1-ON+w}$	3.3	10.2	−55.5	−12.7
$\text{uke2-out+w}$	7.1	9.4	−45.0	−12.9
$\text{uke2-O+w}$	1.4	7.6	−51.0	−15.1
$\text{uke2-N+w}$	n.s.	12.0	n.s.	−9.1
$\text{uke2-ON+w}$	6.8	7.6	−48.3	−16.5

<sup>a</sup>n.s. not stable structure (see the text). <sup>b</sup>Relative energy  $\Delta E_{\text{ZPE}}$  of  $-6.3$  kcal/mol was calculated for the  $\text{U-Ca}^{2+}$  complex (ref 21).

ones in Table S3, Supporting Information). Surprisingly, the larger differences between the metals are in electrostatic rather than in orbital interactions (Table S3, Supporting Information). In solution, interaction energies of some structures with a highly distorted hydration shell are even higher for  $\text{Ca}^{2+}$  than those for  $\text{Mg}^{2+}$ .

In the  $\text{U+M}$  system, the complexes of the rare keto–enol tautomers  $\text{uke1(2)-ON}$  are much less stabilized by the  $\text{Ca}^{2+}$  ion than by the  $\text{Mg}^{2+}$  ion. After inclusion of the first hydration shell ( $\text{U+M+6W}$  system), all  $\text{Ca}^{2+}$  complexes of the rare keto–



enol uke1(2) tautomers are less stable than the canonical uc—O +w structure. In the gas phase, we were not able to optimize stable uke1(2)—N+w<sup>Ca</sup> structures, which were converted spontaneously to uke1(2)—ON+w<sup>Ca</sup> structures. This refers to a low affinity of Ca<sup>2+</sup> for N3.

## CONCLUSIONS

In this contribution, the influence of the environment of the Mg<sup>2+</sup> ion on the specificity of its binding to uracil is discussed and evaluated. On the basis of the gas-phase and solvent-phase results, we have chosen three structures for a detailed analysis, (1) the diketo tautomer with the O4 metal's binding site and (2 and 3) the two keto—enol tautomers with the N3—O2(keto) bidentate metal's binding site as the representatives of the canonical and rare tautomers, respectively. An explicit inclusion of the first coordination shell and implicit description of the bulk environment is necessary to obtain biologically relevant results. In the gas phase, the bidentate N3—Mg—O(keto) binding motif is strongly preferred, stabilizing the rare keto—enol tautomers. On the other hand, the water environment and/or presence of the phosphate group clearly stabilize the canonical diketo tautomer with oxygen atoms as the only metal's binding targets. Thus, the environment has a protective function against point mutations.

Keto oxygens in uracil are weak nucleophiles because a substitution of a water ligand for the O2/O4 keto oxygen is connected with an exergonicity of max. 2.0 kcal/mol (Tables 1 and 4). Therefore, a similar probability of the inner- and outer-sphere binding by the Mg<sup>2+</sup> ion can be expected.

## ASSOCIATED CONTENT

### Supporting Information

Table S1 with schematic drawings of the optimized complexes of uracil with the bare Mg<sup>2+</sup> ion. Their relative and interaction energies are also given and compared with energies of corresponding structures of the thymine—bare Mg<sup>2+</sup> ion system. Relative energies of the Mg<sup>2+</sup> complexes of uken (*n* = 3–6) tautomers are given in Table S2. For the Mg<sup>2+</sup> complexes, the energy decomposition analysis of gas-phase optimized structures of the U+M+6W and U+M+5W+P systems, electron densities at BCPs of gas-phase and solvent-phase optimized structures, and NBO charges of the fragments in gas-phase and solvent-phase optimized structures are shown in Tables S3–S5. For the Ca<sup>2+</sup> complexes, the energy decomposition analysis of the gas-phase optimized structures of the metal complexes of the U+M+6W system are given in Table S3. This material is available free of charge via the Internet at <http://pubs.acs.org>.

## AUTHOR INFORMATION

### Corresponding Author

\*E-mail: [chval@jcu.cz](mailto:chval@jcu.cz).

### Notes

The authors declare no competing financial interest.

## ACKNOWLEDGMENTS

This project was supported by grants from the Czech Science Foundation (204/09/J010) and from the Ministry of Education, Youth and Sports of the Czech Republic (ME09062). The access to the MetaCentrum supercomputing facilities (Grant LM2010005) is highly appreciated.

## REFERENCES

- (1) Florián, J.; Leszczynski, J. *J. Am. Chem. Soc.* **1996**, *118*, 3010–3017.
- (2) Bregadze, V. G.; Gelagutashvili, E. S.; Tsakadze, K. J.; Melikishvili, S. Z. *Chem. Biodiversity* **2008**, *5*, 1980–1989.
- (3) Šponer, J.; Šponer, J. E.; Gorb, L.; Leszczynski, J.; Lippert, B. *J. Phys. Chem. A* **1999**, *103*, 11406–11413.
- (4) Torigoe, H.; Ono, A.; Kozasa, T. *Chem.—Eur. J.* **2010**, *16*, 13218–13225.
- (5) Benda, L.; Straka, M.; Tanaka, Y.; Sychrovský, V. *Phys. Chem. Chem. Phys.* **2011**, *13*, 100–103.
- (6) Miyachi, H.; Matsui, T.; Shigeta, Y.; Yamashita, K.; Hirao, K. *Chem. Phys. Lett.* **2010**, *495*, 125–130.
- (7) Hanus, M.; Kabeláč, M.; Rejnek, M.; Ryjáček, F.; Hobza, P. *J. Phys. Chem. B* **2004**, *108*, 2087–2097.
- (8) Kwiatkowski, J. S.; Bartlett, R. J.; Person, W. B. *J. Am. Chem. Soc.* **1988**, *110*, 2353–2358.
- (9) Colominas, C.; Luque, F. J.; Orozco, M. *J. Am. Chem. Soc.* **1996**, *118*, 6811–6821.
- (10) Kabeláč, M.; Hobza, P. *Phys. Chem. Chem. Phys.* **2007**, *9*, 903.
- (11) Kryachko, E. S.; Nguyen, M. T.; Zeegers-Huyskens, T. *J. Phys. Chem. A* **2001**, *105*, 1288–1295.
- (12) Leszczynski, J. *J. Phys. Chem.* **1992**, *96*, 1649–1653.
- (13) Kabeláč, M.; Hobza, P. *J. Phys. Chem. B* **2006**, *110*, 14515–14523.
- (14) Kosenkov, D.; Gorb, L.; Shishkin, O. V.; Šponer, J.; Leszczynski, J. *J. Phys. Chem. B* **2008**, *112*, 150–157.
- (15) Rejnek, J.; Hanus, M.; Kabeláč, M.; Ryjáček, F.; Hobza, P. *Phys. Chem. Chem. Phys.* **2005**, *7*, 2006.
- (16) Trygubenko, S. A.; Bogdan, T. V.; Rueda, M.; Orozco, M.; Luque, F. J.; Šponer, J.; Slaviček, P.; Hobza, P. *Phys. Chem. Chem. Phys.* **2002**, *4*, 4192–4203.
- (17) Jang, Y. H.; Goddard, W. A.; Noyes, K. T.; Sowers, L. C.; Hwang, S.; Chung, D. S. *J. Phys. Chem. B* **2003**, *107*, 344–357.
- (18) Burda, J. V.; Šponer, J.; Leszczynski, J. *J. Biol. Inorg. Chem.* **2000**, *5*, 178–188.
- (19) Rincón, E.; Yáñez, M.; Toro-Labbé, A.; Mó, O. *Phys. Chem. Chem. Phys.* **2007**, *9*, 2531–2537.
- (20) Marino, T.; Mazzuca, D.; Toscano, M.; Russo, N.; Grand, A. *Int. J. Quantum Chem.* **2007**, *107*, 311–317.
- (21) Russo, N.; Toscano, M.; Grand, A. *J. Phys. Chem. A* **2003**, *107*, 11533–11538.
- (22) Lamsabhi, A. M.; Mó, O.; Yáñez, M.; Boyd, R. J. *J. Chem. Theory Comput.* **2008**, *4*, 1002–1011.
- (23) Lippert, B.; Gupta, D. *Dalton Trans.* **2009**, 4619.
- (24) Burda, J. V.; Šponer, J.; Leszczynski, J.; Hobza, P. *J. Phys. Chem. B* **1997**, *101*, 9670–9677.
- (25) Šponer, J.; Sabat, M.; Burda, J. V.; Leszczynski, J.; Hobza, P. *J. Phys. Chem. B* **1999**, *103*, 2528–2534.
- (26) Poater, J.; Sodupe, M.; Bertran, J.; Solà, M. *Mol. Phys.* **2005**, *103*, 163–173.
- (27) Cerón-Carrasco, J. P.; Jacquemin, D. *ChemPhysChem* **2011**, *12*, 2615–2623.
- (28) Ono, A.; Torigoe, H.; Tanaka, Y.; Okamoto, I. *Chem. Soc. Rev.* **2011**, *40*, 5855–5866.
- (29) Martínez, A. *J. Phys. Chem. A* **2009**, *113*, 1134–1140.
- (30) Wang, N.; Li, P.; Hu, Y.; Bu, Y.; Wang, W.; Xie, X. *J. Theor. Comput. Chem.* **2007**, *06*, 197.
- (31) Rincón, E.; Jaque, P.; Toro-Labbé, A. *J. Phys. Chem. A* **2006**, *110*, 9478–9485.
- (32) Gutlé, Salpin, J.; Cartailier, T.; Tortajada, J.; Gaigeot, M. *J. Phys. Chem. A* **2006**, *110*, 11684–11694.
- (33) Li, D.; Ai, H. *J. Phys. Chem. B* **2009**, *113*, 11732–11742.
- (34) Gillis, E. A. L.; Rajabi, K.; Fridgen, T. D. *J. Phys. Chem. A* **2009**, *113*, 824–832.
- (35) Marino, T.; Toscano, M.; Russo, N.; Grand, A. *Int. J. Quantum Chem.* **2004**, *98*, 347–354.
- (36) Noguera, M.; Bertran, J.; Sodupe, M. *J. Phys. Chem. A* **2004**, *108*, 333–341.

- (37) Pavelka, M.; Shukla, M. K.; Leszczynski, J.; Burda, J. V. *J. Phys. Chem. A* **2008**, *112*, 256–267.
- (38) Pavelka, M.; Šimánek, M.; Šponer, J.; Burda, J. V. *J. Phys. Chem. A* **2006**, *110*, 4795–4809.
- (39) Noguera, M.; Bertran, J.; Sodupe, M. *J. Phys. Chem. B* **2008**, *112*, 4817–4825.
- (40) Lamsabhi, A. M.; Alcamí, M.; Mó, O.; Yáñez, M.; Tortajada, J. *J. Phys. Chem. A* **2006**, *110*, 1943–1950.
- (41) Sigel, R.; Sigel, H. *Acc. Chem. Res.* **2010**, *43*, 974–984.
- (42) van der Wijst, T.; Fonseca Guerra, C.; Swart, M.; Bickelhaupt, F. M.; Lippert, B. *Chem.—Eur. J.* **2009**, *15*, 209–218.
- (43) Lippert, B. *Prog. Inorg. Chem.* **1989**, *37*, 1–97.
- (44) Lamsabhi, A. M.; Alcamí, M.; Mó, O.; Yáñez, M.; Tortajada, J. *ChemPhysChem* **2004**, *5*, 1871–1878.
- (45) Lamsabhi, A. M.; Alcamí, M.; Mó, O.; Yáñez, M.; Tortajada, J.; Salpin, J. Y. *ChemPhysChem* **2007**, *8*, 181–187.
- (46) Odani, A.; Kozłowski, H.; Swiatek-Kozłowska, J.; Brasun, J.; Opershall, B. P.; Sigel, H. *J. Inorg. Biochem.* **2007**, *101*, 727–735.
- (47) Hu, X. B.; Li, H. R.; Zhang, L.; Han, S. J. *J. Phys. Chem. B* **2007**, *111*, 9347–9354.
- (48) Schoellhorn, H.; Thewalt, U.; Lippert, B. *J. Am. Chem. Soc.* **1989**, *111*, 7213–7221.
- (49) Eizaguirre, A.; Lamsabhi, A. M.; Mó, O.; Yáñez, M. *Theor. Chem. Acc.* **2010**, *128*, 457–464.
- (50) Russo, N.; Sicilia, E.; Toscano, M.; Grand, A. *Int. J. Quantum Chem.* **2002**, *90*, 903–909.
- (51) Trujillo, C.; Lamsabhi, A. M.; Mó, O.; Yáñez, M.; Salpin, J.-Y. *Org. Biomol. Chem.* **2008**, *6*, 3695–3702.
- (52) Eizaguirre, A.; Mó, O.; Yáñez, M.; Boyd, R. J. *Org. Biomol. Chem.* **2010**, *9*, 423–431.
- (53) Salpin, J.-Y.; Guillaumont, S.; Ortiz, D.; Tortajada, J.; Maitre, P. *Inorg. Chem.* **2011**, *50*, 7769–7778.
- (54) Schaftenaar, G.; Noordik, J. *J. Comput.-Aided Mol. Des.* **2000**, *14*, 123–134.
- (55) Frisch, M. J. et al. *Gaussian 09*, revision A.01; Gaussian, Inc.: Pittsburgh, PA, 2009.
- (56) Keith, T. A. *AIMAll*, version 10.11.24. <http://aim.tkgristmill.com> (2010).
- (57) Boys, S. F.; Bernardi, F. *Mol. Phys.* **1970**, *19*, 553–566.
- (58) Zimmermann, T.; Chval, Z.; Burda, J. V. *J. Phys. Chem. B* **2009**, *113*, 3139–3150.
- (59) ADF2010, *SCM, Theoretical Chemistry*; Vrije Universiteit: Amsterdam, The Netherlands, 2010.
- (60) Ziegler, T.; Rauk, A. *Theor. Chim. Acta* **1977**, *46*, 1–10.
- (61) Ziegler, T.; Rauk, A. *Inorg. Chem.* **1979**, *18*, 1755–1759.
- (62) Mitoraj, M.; Michalak, A.; Ziegler, T. *J. Chem. Theory Comput.* **2009**, *5*, 962–975.
- (63) Mitoraj, M. P.; Michalak, A.; Ziegler, T. *Organometallics* **2009**, *28*, 3727–3733.
- (64) Mitoraj, M. P.; Kurczab, R.; Boczar, M.; Michalak, A. *J. Mol. Model.* **2010**, *16*, 1789–1795.
- (65) Wu, R.; McMahon, T. B. *J. Am. Chem. Soc.* **2006**, *129*, 569–580.
- (66) Millefiori, S.; Alparone, A. *Chem. Phys.* **2004**, *303*, 27–36.
- (67) As a minimal model for a solvated ion, see: Deerfield, D. W.; Fox, D. J.; Head-Gordon, M.; Hiskey, R. G.; Pedersen, L. G. *J. Am. Chem. Soc.* **1991**, *113*, 1892–1899.
- (68) Šponer, J. E.; Sychrovský, V.; Hobza, P.; Šponer, J. *J. Phys. Chem. Chem. Phys.* **2004**, *6*, 2772–2780.
- (69) Hu, X.; Li, H.; Liang, W.; Han, S. J. *J. Phys. Chem. B* **2004**, *108*, 12999–13007.
- (70) Hu, X.; Li, H.; Liang, W.; Han, S. J. *J. Phys. Chem. B* **2005**, *109*, 5935.
- (71) Fan, J.; Shang, Z.; Liang, J.; Liu, X.; Jin, H. *J. Mol. Struct.: THEOCHEM* **2010**, *939*, 106–111.
- (72) Kryachko, E. S.; Nguyen, M. T.; Zeegers-Huyskens, T. *J. Phys. Chem. A* **2001**, *105*, 1934.
- (73) Rincón, E.; Toro-Labbé, A. *Chem. Phys. Lett.* **2007**, *438*, 93–98.
- (74) Freisinger, E.; Sigel, R. K. O. *Coord. Chem. Rev.* **2007**, *251*, 1834–1851.
- (75) Rulíšek, L.; Šponer, J. *J. Phys. Chem. B* **2003**, *107*, 1913–1923.